Cardiovascular Research (2016) **111**, 56–65
doi:10.1093/cvr/cvw078

The H19 long noncoding RNA is a novel negative regulator of cardiomyocyte hypertrophy

Lantao Liu[1], Xiangbo An[2], Zhenhua Li[1], Yao Song[2], Linling Li[3], Song Zuo[3], Nian Liu[3], Guan Yang[1], Haijing Wang[1], Xuan Cheng[1], Youyi Zhang[2]*, Xiao Yang[1]*, and Jian Wang[1]*

[1]State Key Laboratory of Proteomics, Collaborative Innovation Center for Cardiovascular Disorders, Genetic Laboratory of Development and Disease, Institute of Biotechnology, 20 Dongdajie, Beijing 100071, China; [2]Institute of Vascular Medicine, Peking University Third Hospital and Key Laboratory of Molecular Cardiovascular Sciences, Ministry of Education, Key Laboratory of Cardiovascular Molecular Biology and Regulatory Peptides, Ministry of Health, 49 Huayuan-Bei Road, Beijing 100191, China; and [3]Department of Cardiology, Beijing Anzhen Hospital, Capital Medical University, National Clinical Research Center for Cardiovascular Diseases, Beijing, China

Received 3 June 2015; revised 31 March 2016; accepted 8 April 2016; online publish-ahead-of-print 15 April 2016

Time for primary review: 29 days

Aims The H19 lncRNA, a highly abundant and conserved imprinted gene, has been implicated in many essential biological processes and diseases. However, the function of H19 in the heart remains unknown. In this study, we investigated the function and underlying mechanism of H19 in regulating cardiomyocyte hypertrophy.

Methods and results We first detected the expression of H19 and its encoded miR-675 in both normal and diseased hearts and verified their up-regulations in pathological cardiac hypertrophy and heart failure. Adenovirus-mediated expression and a siRNA-mediated silence of H19 showed that H19 overexpression reduced cell size both at baseline and in response to phenylephrine, whereas knock-down of H19 induced cardiomyocyte hypertrophy. Overexpression or knock-down of miR-675 in cardiomyocytes demonstrated that miR-675 also inhibited cardiomyocyte hypertrophy. Moreover, inhibition of miR-675 reversed the reduction of cardiomyocyte size in H19-overexpressing cardiomyocytes, while infection with an adenovirus carrying H19 fragment without pre-miR-675 (H19-Tru) or with mutant sequences of pre-miR-675 (H19-Mut) failed to reduce cardiomyocyte size, indicating that miR-675 mediated the inhibitory effect of H19 on cardiomyocyte hypertrophy. We also identified that CaMKIIδ was a direct target of miR-675 and partially mediated the effect of H19 on cardiomyocyte hypertrophy. Furthermore, *in vivo* silencing of miR-675 using a specific antagomir in a pressure overload-induced mouse model of heart failure increased cardiac CaMKIIδ expression and exacerbated cardiac hypertrophy.

Conclusion These findings reveal a novel function of H19-miR-675 axis targeting CaMKIIδ as a negative regulator of cardiac hypertrophy, suggesting its potential therapeutic role in cardiac diseases.

Keywords Long noncoding RNA • H19 • miR-675 • Cardiac hypertrophy • CaMKIIδ

1. Introduction

Cardiac hypertrophy is an adaptive reaction of the heart against various stresses to maintain cardiac function at the early stage. However, sustained cardiac hypertrophy with maladaptive cardiac remodelling often leads to increased risk for heart failure and cardiac death.[1,2] Although a variety of specific peptide hormones, growth factors, and miRNAs have been identified as the regulators of cardiac hypertrophy,[3,4] the underlying molecular mechanisms of cardiac hypertrophy are still not fully understood.

Long non-coding RNAs (lncRNAs) are transcribed RNA molecules >200 nucleotides in length, but have no potential of protein-coding.[5] LncRNAs have been shown to play important roles in various physiological processes, such as RNA processing, modulation of apoptosis and invasion, chromatin modification, and as a competing endogenous RNA (ceRNA).[6–8] Recent studies have indicated that lncRNAs also function in heart development and diseases,[9–12] while only a limited number of lncRNAs have been identified as the regulators of cardiac hypertrophy. For example, cardiac hypertrophy related factor is shown to regulate cardiac hypertrophy by targeting miR-489.[13] Myosin heavy chain-associated RNA transcript (Mhrt), a cardiac-specific lncRNA, has been demonstrated to protect the heart from pathological cardiac hypertrophy.[14] Therefore, further investigation on function of lncRNAs in cardiac hypertrophy is necessary for better understanding the regulation of cardiac homeostasis.

* Corresponding author. Tel/fax: +86 10 63895937, E-mail: yangx@bmi.ac.cn (X.Y); Tel/fax: +86 10 63895937, E-mail: wangjian7773@126.com (J.W); Tel/fax: +86 10 82802306, E-mail: zhangyy@bjmu.edu.cn (Y.Z.)

As one of the first identified imprinted genes, the lncRNA H19 gene has been verified as an important regulator in mammalian development and diseases.[15,16] Exon 1 of H19 carries a miRNA containing hairpin, which has been found to act as the template for miR-675, and it has been shown that miR-675 can confer functionality on H19.[17–19] A series of RNA-seq data from pathological cardiac remodelling have indicated that H19 is always up-regulated in hypertrophic hearts,[20–22] suggesting its possible role in cardiac hypertrophy. Until now, the exact function of H19 in the heart is rarely known. In this study, we provided the first evidence to show that H19 could inhibit the hypertrophic growth of cardiomyocytes, suggesting a novel function of H19 as a negative regulator of cardiac hypertrophy.

2. Methods

2.1 Transverse aortic constriction

Transverse aortic constriction (TAC) surgeries were performed on male C57BL/6 mice (8 weeks old). The mice were anaesthetized with 2.0% isoflurane (v/v) in 45 mL/min oxygen flow. After thoracotomy, the transverse thoracic aorta was dissected, and a 6-0 silk suture was tied around the aorta against a 26-gauge needle. The sham groups underwent a sham operation involving thoracotomy and aortic dissection without constriction of the aorta. Animals were sacrificed by cervical dislocation, and the hearts were harvested for analysis. The experiments were performed according to the protocols approved by the Animal Experiment Committee of the Institute of Biotechnology and conformed to the US National Institutes of Health Guide for the Care and Use of Laboratory Animals.

2.2 Isolation, culture, and treatment of cardiomyocytes

Neonatal ventricular myocytes were isolated from 2-day-old pups, infected, and stained as described.[23] In brief, a central thoracotomy was performed after the neonatal mice were deeply anaesthetized with 1.0% isoflurane. The hearts were washed and minced in sodium bicarbonate-, Ca^{2+}-, and Mg^{2+}-free Hanks balanced salt solution (D-Hanks). Tissues were then dispersed in a series of incubations at 37°C in D-Hanks buffered solution containing 1.2 mg/mL pancreatin and 0.14 mg/mL collagenase (Worthington, USA). After centrifugation, the cells were suspended in Dulbecco's modified Eagle medium/F-12 (GIBCO, USA) containing 10% heat-inactivated foetal bovine serum, 100 U/mL penicillin, 100 mg/mL streptomycin, and 0.1 mM bromodeoxyuridine. The dissociated cells were pre-plated at 37°C for 1 h to separate cardiomyocytes by adherence of cardiac fibroblasts. The cardiomyocytes were collected and diluted to 1×10^6 cells/mL and plated in 1% gelatin-coated different culture dishes. Neonatal cardiomyocytes were incubated at 37°C and 5% CO_2 in a humidified chamber. After 48 h of culture, the various treatments were performed.

Adult mouse cardiac myocytes were isolated as described.[24] The dissociated cells were pre-plated at 37°C for 1 h to separate cardiomyocytes by adherence of cardiac fibroblasts.

2.3 Cell immunostaining

Immunostaining was carried out mainly as described.[25] Cardiomyocytes were fixed with 4% formaldehyde for 30 min at 4°C and then treated with 0.5% Triton-X 100 in PBS for 5 min at room temperature. After that, cells were incubated with primary antibody against α-actinin (Sigma, USA, Lot No. A7811) at 4°C overnight, followed by incubation with fluorescence-conjugated secondary antibody. Photo capture was performed using a Nikon laser microscope (Eclipse E600, Nikon Instruments Inc., Japan). For each sample, more than five fields covering the whole slide were picked and counted.

2.4 Generation of adenovirus expressing wild type of H19 and H19 with deleted or mutant pre-miR-675 sequence

H19 cDNA was PCR-amplified from cDNA fragments of mouse hearts and inserted into the adenoviral vectors. The primers were as following: H19 sense: 5′-TTTCTCGAGACCGGGTGTGGGAGGGGGGT-3′; H19 antisense: 5′-TTTTCTAGA GACTGTAACTGTATTTATTGA-3′.

To generate truncation of H19 without pre-miR-675, the two fragments were amplified separately using the primers as following: H19-Tru sense: 5′-TTTAGATCTACCGGGTGTGGGAGGGGGGT-3′; H19-Tru mid-antisense: 5′-TTTGTCGACGTGCCTCATGGGAATGGTGTG-3′; and H19-Tru mid-sense: 5′-TTTGTCGACTGACAGACAGAACATTTCC AG-3′; H19-Tru antisense: 5′-TTTTCTAGAGACTGTAACTGTATTT ATTG A-3′, and then were ligated and inserted into the adenoviral vectors.

To generate H19 with mutant pre-miR-675, the sequences were changed as follows: TGGTGCGGAAAGGGCCCACAGT was changed to CCACATTTCAAGGGCCCACAGT, and CTGTATGCCCTAACCGCT CAGT was changed to CCACATCGCCATACCGCTCAGT.[26]

2.5 Cloning of CaMKIIδ 3′-UTR and luciferase reporter assay

For target assay, we performed luciferase reporter experiments in the HEK293 cells. The 3′-UTR fragment of CaMKIIδ was amplified using primers: 5′-TTTCTCGAGAGCGTTACCTCCACCA-3′ and 5′-TTTACGCG TGATCACAGACTGCAAG-3′, and cloned into pGL3-CM luciferase reporter vector. The construct (Luc-CaMKIIδ mutant) containing a mutated CaMKIIδ-UTR (GCATACA was mutated to GAATTC) was also constructed. For luciferase assay, reporter plasmids were co-transfected using lipofectamine 2000 reagent (Invitrogen, USA, Lot No.11668-019). The phRG-TK vector (Promega, USA) that expresses a synthetic renilla luciferase was used for normalizing transfection efficiency. After transfection, luciferase activities were measured with a dual luciferase reporter assay kit (Invitrogen, USA, Lot No. E1910) using LB 960 Centro XS3 luminometer (Berthold Technologies, GmbH & Co. KG, Germany).[27]

2.6 Western blot

Western blots were carried out on myocardial extracts as described.[28] Proteins (30 μg) were electrophoresed on SDS-PAGE and transferred onto PVDF membranes. Immunoblotting was performed according to manufacturer's instructions using the following antibodies: caMKIIδ (Abcam, UK, Lot No. EPR13095), GAPDH (ZhongShanJinQiao, China, Lot No. TA-08), HDAC4 (Cell Signaling, USA, Lot No. #5392), and p-HDAC4 (Cell Signaling, USA, Lot No. #3424).

2.7 Real-time PCR

Total RNA was isolated from heart tissues and neonatal cardiomyocytes using TRIzol Reagent (Invitrogen, USA), cDNA was synthesized using SuperRT One Step RT–PCR Kit (CWBIO, China) and subjected to real-time PCR using SYBR Green Real-time PCR Master Mix (TOYOBO, Japan) with 7500 Fast Real-Time PCR System (Applied Biosystems, USA), and GAPDH was used as a reference gene. The following primers were used: GAPDH, 5′-TGCCCAGAACATCATCCCT-3′ and 5′-GGTCCTCA GTGTAGCCCAAG-3′; ANF, 5′-GCCGGTAGAAGATGAGGTCA-3′ and 5′-GGGCTCCAATCCTGTCAATC-3′; SKA, 5′-GGCTCCCAGCACC ATGAAGA-3′ and 5′-CAGCACGATTGTCGATTGTCG-3′; β-MHC, 5′-GTGAAGGGCATGAGGAAGAGT-3′ and 5′-AGGCCTTCACCTTC AGCT GC-3′; BNP, 5′-GCTCTTGAAGGACCAAGGCCTCAC-3′ and 5′-GATCCGA TCCGG TCTATCTTGTGC-3′; CaMKIIδ, 5′-GAATC TGCCGTCTCTTGAA-3′ and 5′-TCTCTTG CCACTATGTCTTC-3′.

MiRNA real-time PCR was performed with miR-specific primers from the TaqMan miR assays (Applied Biosystems, USA) in the 7500 Fast Real-time PCR System (Applied Biosystems, USA) according to manufacturer's protocol, and U6 was used as a reference gene.

2.8 Northern blot

Total RNA was isolated using TRIzol reagent (Invitrogen, Carlsbad, CA, USA). RNA quality was assessed by 1% agarose gel electrophoresis in the presence of ethidium bromide. Northern blot analysis was performed as described using 30 μg total RNA from each sample.[25] Probes were synthesized in Invitrogen Biotechnology Co., Ltd. (Beijing, China) as following: miR-675-3p, 5′-ACTGAGCGGTTAGGGCATACAG-3′; and U6 probe, 5′-CGAATTTGCGTGTCATCCTTGCG-3′, was served as a loading control. Probes were labelled with ^{32}P γ-ATP using T4 polynucleotide kinase (New England Biolabs, Inc., Ipswich, MA, USA).

2.9 Antagomir application on TAC models

TAC surgeries were performed on male C57BL/6 mice (8 weeks old) as described. Chemically modified antisense oligonucleotides (antagomir) were synthesized by GenePharma Co. Ltd. (Suzhou, China) Treatments started 1 week after TAC, and animals received 0.2 mL saline, antagomir-675 (3 injections, 30 mg per kg body weight) via tail vein injections.

2.10 Histology and immunohistology

Heart tissues were fixed in 4% PFA at 4°C overnight, embedded in paraffin, and sectioned at 5 μm. Sections were stained with haematoxylin and eosin (H&E), Masson trichrome, and laminin antibody (ZhongShanJinQiao, China, Lot No. ZA-0351) as standard protocols.

2.11 Statistical analysis

All statistical analyses were performed using SPSS software. Results are means ± SEM. Statistical differences between two groups were determined by Student's *t*-test, and statistical differences among more than two groups were determined by ANOVA followed by SNK-q method. *P*-values of <0.05 were considered significant.

3. Results

3.1 H19 and its encoded miR-675 are up-regulated in pathological cardiac hypertrophy

To identify whether H19 was altered in cardiac diseases, we first detected H19 RNA level in a mouse model of cardiac hypertrophy induced by TAC. Consistent with the previously reported RNA-seq data,[20–22] we found H19 RNA level was significantly up-regulated in hypertrophic hearts (*Figure 1A*; see Supplementary material online,

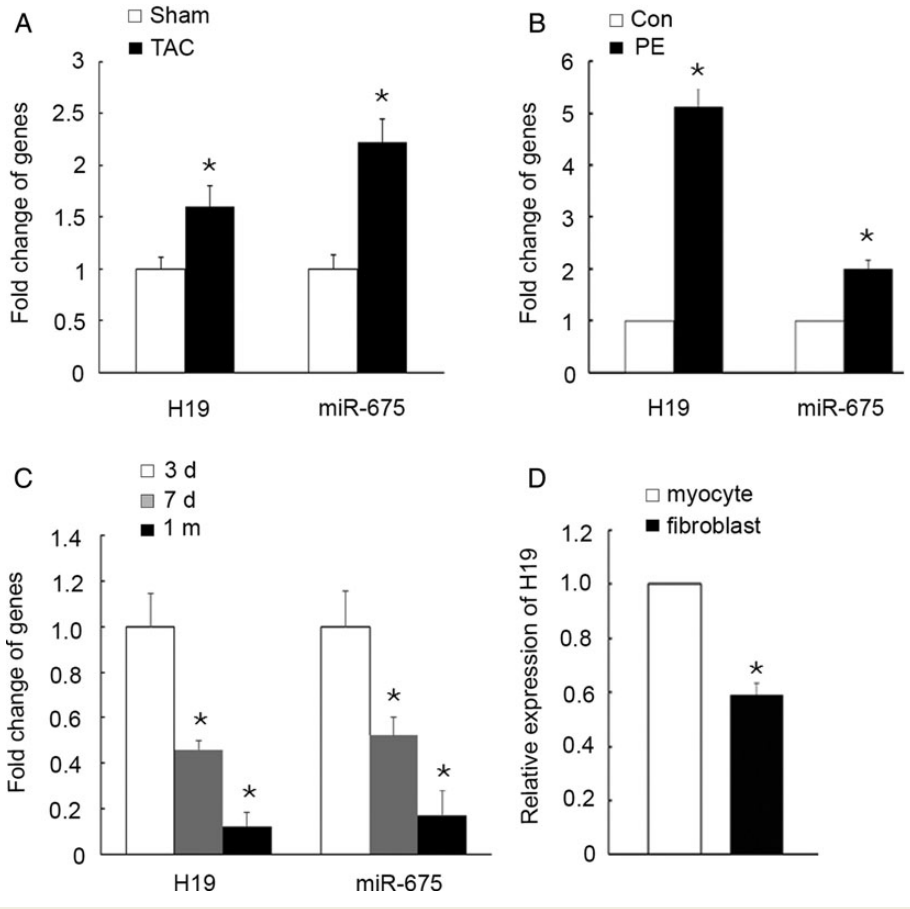

Figure 1 H19 and its encoded miR-675 were up-regulated in pathological cardiac hypertrophy. (*A*) Detection of H19 and miR-675 levels in heart samples from sham- and TAC-treated mice by real-time PCR. $n = 3$ independent experiments, $^*P < 0.05$ vs. sham group. (*B*) Detection of H19 and miR-675 levels in PE-treated cardiomyocytes by real-time PCR. $n = 5$ independent experiments, $^*P < 0.05$ vs. control group. (*C*) The expression levels of H19 and miR-675 during heart maturation after birth were detected by real-time PCR. $n = 5$ independent experiments, $^*P < 0.05$. (*D*) Expression levels of H19 in cardiomyocytes and cardiac fibroblasts were detected by real-time PCR. Data represent means ± SEM. $n = 3$ independent experiments, $^*P < 0.05$.

Figure S5A and *E*). Phenylephrine (PE) has been well documented to induce cardiac hypertrophy. The H19 expression level was also found to be up-regulated in PE-treated cardiomyocytes (*Figure 1B*). Since H19 encodes miR-675-3p and miR-675-5p,[17–19] and miR-675-3p is more abundant than miR-675-5p as seen from miRBase, we detected the expression of miR-675-3p (hereinafter referred to as miR-675) and found that it was also up-regulated under these pathological conditions (*Figure 1A* and *B*; see Supplementary material online, *Figures S1A* and *B* and *S5B* and *F*). Moreover, H19 and miR-675 were found to be up-regulated in human heart failure samples (see Supplementary material online, *Figure S1C*) but decreased in mouse model of physiological cardiac hypertrophy induced by tread-mill training (see Supplementary material online, *Figure S1D*). The expressions of H19 and miR-675 during postnatal heart maturation were found to be gradually down-regulated with ages after birth (*Figure 1C*). Detection of H19 in different cardiac cells showed that H19 was more abundant in myocytes than fibroblasts (*Figure 1D*). All these data suggested that H19 and its encoded miR-675 may participate in the development of pathological cardiac hypertrophy.

3.2 H19 inhibits the hypertrophic growth of cardiomyocytes

To determine the role of H19 in cardiac hypertrophy, we overexpressed H19 in neonatal cardiomyocytes using an adenovirus that contained mouse H19 (Ad-H19). Infection of Ad-H19 in cardiomyocytes successfully increased the expressions of H19 and miR-675 (*Figure 2A*; see Supplementary material online, *Figure S2A* and *B*). The cardiomyocytes infected with adenoviruses for 48 h were immunostained for α-actinin to study the morphological changes. Immunostaining revealed

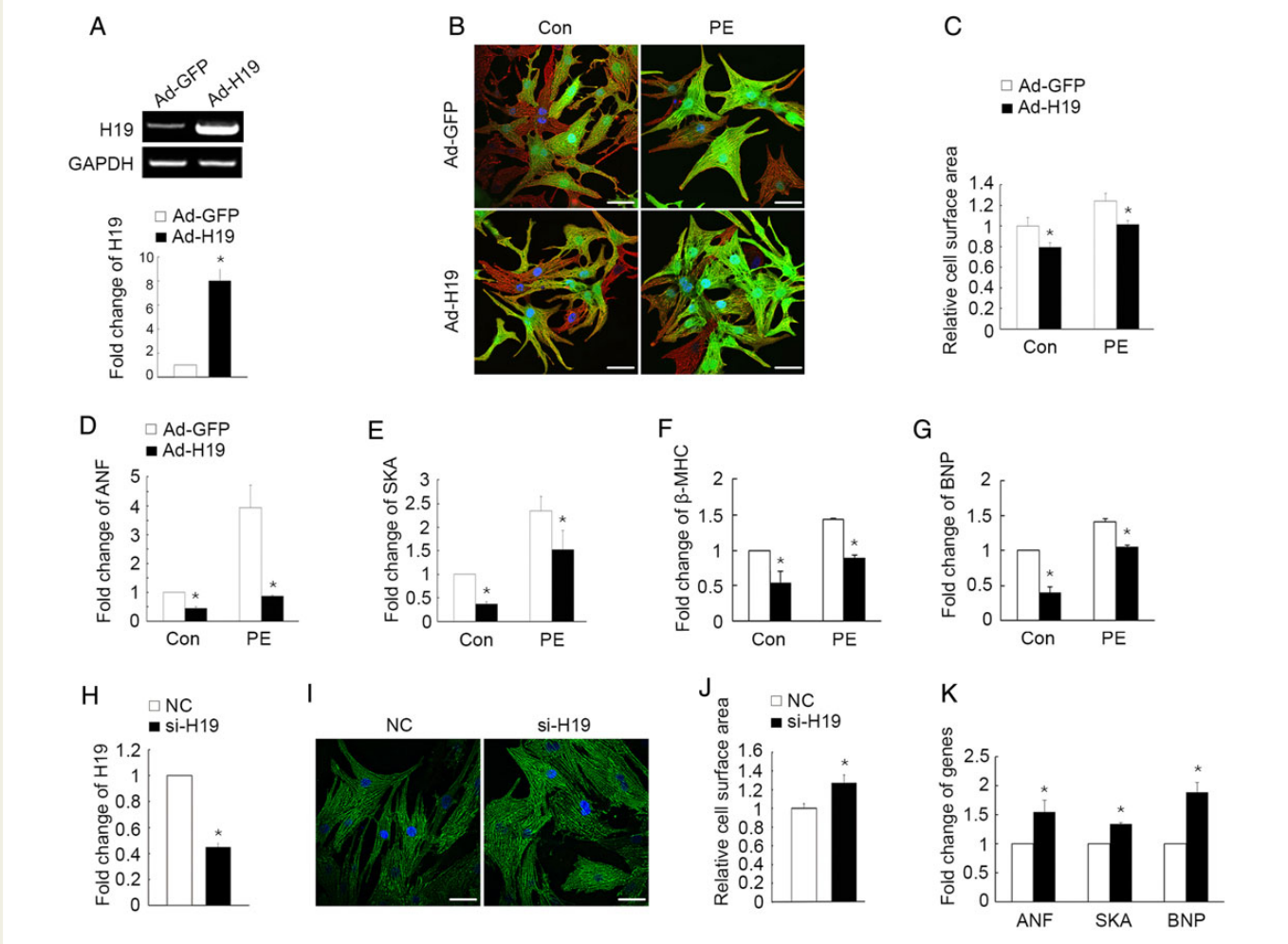

Figure 2 H19 inhibited the hypertrophic growth of cardiomyocytes. (*A*) RT–PCR and quantitative data showed that H19 adenovirus induced H19 overexpression in cardiomyocytes. (*B*) Isolated neonatal cardiomyocytes were infected with Ad-H19 or control adenovirus and treated with or without PE. Cardiomyocytes were stained for GFP (green) and α-actinin (red). Hoechst staining was done to visualize the nuclei (blue). The scale bar represents 40 μm. (*C*) Fold change in mean cell surface area of α-actinin-immunostained cardiomyocytes (214 cells per condition; $n = 4$). *$P < 0.05$ vs. respective Ad-GFP group. (*D*–*G*) ANF, SKA, β-MHC, and BNP transcripts in different groups were checked by real-time PCR. $n = 5$ independent experiments. *$P < 0.05$ relative to respective Ad-GFP group. (*H*) Real-time PCR showed that si-H19 effectively reduced H19 expression in cardiomyocytes. $n = 5$ independent experiments, *$P < 0.05$. (*I*) Isolated neonatal cardiomyocytes were transfected with si-H19 or NC. Cardiomyocytes were stained for α-actinin (green) and Hoechst (blue). The scale bar represents 40 μm. (*J*) Fold change in mean cell surface area of α-actinin-immunostained cardiomyocytes (237 cells per condition; $n = 4$). *$P < 0.05$. (*K*) ANF, SKA, and BNP transcripts were checked by real-time PCR. Data represent means ± SEM. $n = 5$ independent experiments, *$P < 0.05$.

that PE treatment increased the size of cardiomyocytes, while overexpression of H19 reduced the cell size both at basal condition and in response to PE (*Figure 2B* and *C*). Similarly, the foetal genes such as atrial natriuretic factor (ANF), skeletal muscle and cardiac actin (SKA), β-myosin heavy chain (β-MHC), and brain natriuretic peptide (BNP) were also significantly down-regulated by H19 overexpression both at baseline and in response to PE (*Figure 2D–G*). To further examine the function of endogenous H19, a siRNA for mouse H19 was administered in mouse neonatal cardiomyocytes. Transfection of cardiomyocytes with siRNA-H19 significantly reduced the expressions of endogenous H19 and miR-675 (*Figure 2H*; see Supplementary material online, *Figure S2C*) and increased the cell size (*Figure 2I* and *J*) and mRNA expression of foetal genes at baseline (*Figure 2K*). These data indicated that H19 overexpression is sufficient to inhibit the hypertrophic growth of cardiomyocytes.

3.3 miR-675 inhibits the hypertrophic growth of cardiomyocytes

To test whether miR-675 also played an important role in cardiomyocyte hypertrophy, miR-675 mimics were administered in neonatal cardiomyocytes to induce miR-675 overexpression (see Supplementary material online, *Figure S2D*). The exogenous miR-675 reduced the cell size at baseline and attenuated PE-induced hypertrophic growth of cardiomyocytes, as seen by the morphological analysis and quantification of relative cell surface area (*Figure 3A* and *B*). Consistently, expression levels of ANF, SKA, and β-MHC were also repressed by miR-675 both at baseline and in response to PE (*Figure 3C–E*). We also knocked down endogenous miR-675 in cardiomyocytes using antimiR-675 (see Supplementary material online, *Figure S2E*) and found that inhibition of miR-675 increased the cell size (*Figure 3F* and *G*) and mRNA expression levels of foetal genes at baseline (*Figure 3H*). These data demonstrated that miR-675 could negatively regulate the cardiomyocyte hypertrophy.

3.4 CaMKIIδ is a direct target of miR-675 in cardiomyocytes

Because miR-675 inhibited hypertrophic growth of cardiomyocytes, we anticipated that its target genes would include genes that induced cardiac hypertrophy. Target prediction led to the identification of a pro-hypertrophic factor, Ca/calmodulin-dependent protein kinase IIδ (CaMKIIδ), whose mRNA 3′-UTR region comprised the seed sequences and flanking nucleotides matching miR-675, which was highly

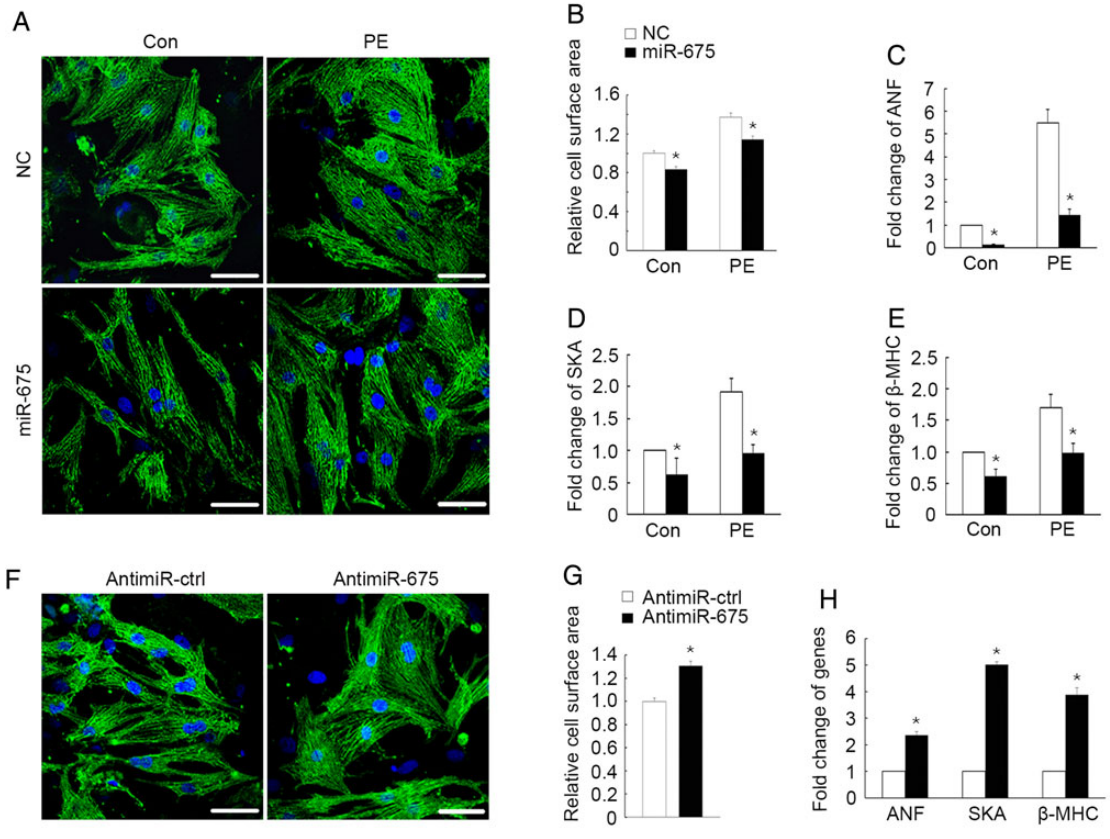

Figure 3 miR-675 inhibited the hypertrophic growth of cardiomyocytes. (*A*) Isolated neonatal cardiomyocytes were transfected with control or miR-675 mimics and treated with or without PE. Cardiomyocytes were stained for α-actinin (green) and Hoechst (blue). The scale bar represents 40 μm. (*B*) Fold change in mean cell surface area of α-actinin-immunostained cardiomyocytes (213 cells per condition; $n = 4$). *$P < 0.05$ vs. respective control group. (*C–E*) ANF, SKA, and β-MHC transcripts were detected by real-time PCR. $n = 5$ independent experiments, *$P < 0.05$ relative to respective control. (*F*) Isolated neonatal cardiomyocytes were transfected with antimiR-ctrl or antimiR-675. Cardiomyocytes were stained for α-actinin (green) and Hoechst (blue). The scale bar represents 40 μm. (*G*) Fold change in mean cell surface area of α-actinin-immunostained cardiomyocytes (215 cells per condition; $n = 4$). *$P < 0.05$. (*H*) Levels of ANF, SKA, and β-MHC were measured by real-time PCR. $n = 5$ independent experiments, *$P < 0.05$.

conserved among different species (*Figure 4A*). To confirm whether CaMKIIδ was a direct target of miR-675, we constructed luciferase reporter gene harbouring the normal or mutant type of 3′-UTR of CaMKIIδ and performed luciferase reporter assays in HEK293 cells. Co-transfection of miR-675 with the luciferase reporter gene linked to the wild-type 3′-UTR of CaMKIIδ strongly inhibited the luciferase activity, while no effect was observed with the construct harbouring a mutant segment of CaMKIIδ 3′-UTR (*Figure 4B*). Consistent with the luciferase results, the CaMKIIδ mRNA and protein levels were all downregulated by transfection of cardiomyocytes with miR-675 (*Figure 4C–E*). In a reciprocal experiment, we inhibited the endogenous miR-675 in cardiomyocytes and observed the increased CaMKIIδ expression both at mRNA and protein levels (*Figure 4C–E*). These results suggested that miR-675 might inhibit cardiomyocyte hypertrophy by targeting CaMKIIδ.

3.5 miR-675 mediates the anti-hypertrophic effect of H19 on cardiomyocytes

Since both H19 and miR-675 could inhibit the hypertrophic growth of cardiomyocytes, we hypothesized that miR-675 might mediate the anti-hypertrophic effect of H19. To test this hypothesis, we first knocked down miR-675 in H19-overexpressing cardiomyocytes by treating the cardiomyocytes with Ad-H19 together with either antimiR-675 or antimiR-ctrl. The results showed that inhibition of miR-675 could reverse the reduction of cardiomyocyte size (*Figure 5A* and *B*) and foetal genes expression induced by H19 overexpression (*Figure 5C–F*). We further detected the expression of CaMKIIδ and HDAC4, whose phosphorylation was induced by CaMKIIδ,[29–31] and found that miR-675 inhibition could also reverse the reduction of CaMKIIδ and phosphorylation of HDAC4 induced by H19 overexpression (*Figure 5G*).

To further test this result, we also generated two adenoviruses containing the fragment of H19 without pre-miR-675 (Ad-H19-Tru) and the mutant type of H19 with mutant sequences of pre-miR-675 (Ad-H19-Mut) to infect neonatal cardiomyocytes. H19 but not miR-675 was successfully overexpressed in cardiomyocytes infected with Ad-H19-Tru or Ad-H19-Mut (see Supplementary material online, *Figure S3A* and *B*). Ectopic expression of these two types of H19 fragments lost the ability to reduce cardiomyocyte size and foetal genes expression (see Supplementary material online, *Figure S3C–H*). All these results suggested that H19-induced suppression of cardiomyocyte hypertrophy was mainly mediated by miR-675.

3.6 CaMKIIδ partially reverses the anti-hypertrophic action of H19 in cardiomyocytes

Since miR-675 mainly mediated the effect of H19 on cardiomyocyte hypertrophy, we then determined whether CaMKIIδ could reverse the inhibitory effect of H19 on cardiomyocyte hypertrophy. We found that overexpression of H19 reduced and inhibition of endogenous H19 induced the expression of CaMKIIδ (*Figure 6A* and *B*), while expression of mutant type of H19 did not alter the expression of CaMKIIδ in

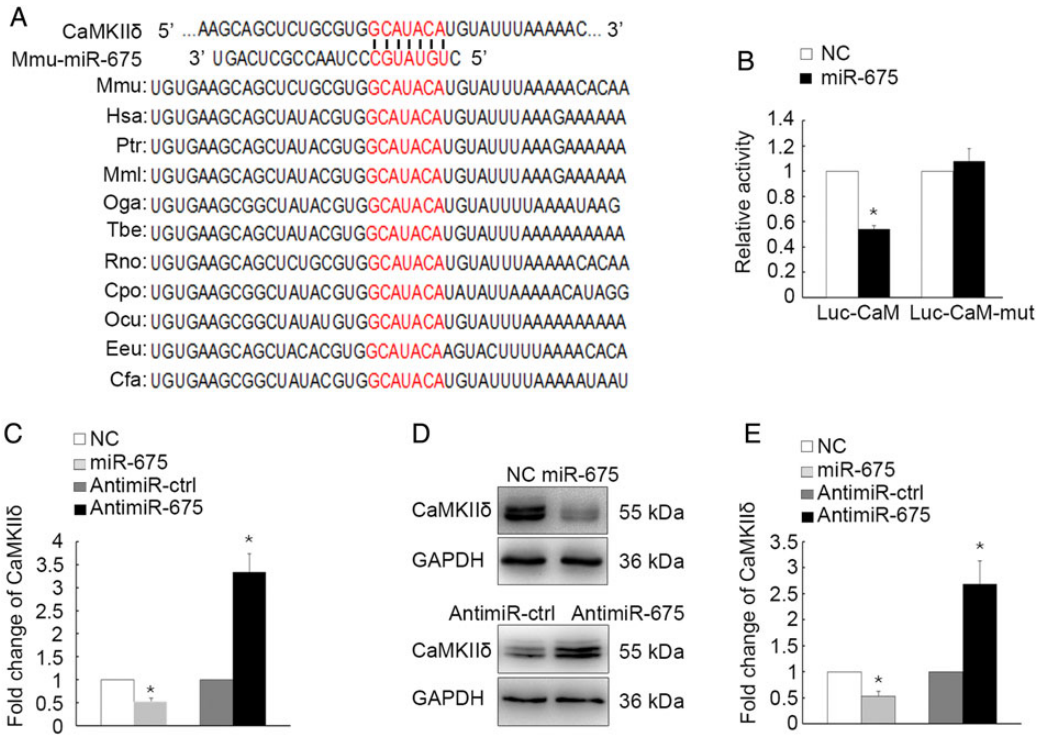

Figure 4 CaMKIIδ was a direct target of miR-675 in cardiomyocytes. (*A*) miR-675 targeted the 3′-UTR of CaMKIIδ mRNA, which is highly conserved among different species. (*B*) Dual luciferase activity assay of HEK293 cells co-transfected with a luciferase reporter plasmid containing the naive or mutant CaMKIIδ 3′-UTR. $n = 5$ independent experiments, $^*P < 0.05$. (*C*) Detection of CaMKIIδ mRNA levels affected by miR-675 using real-time PCR. $n = 5$ independent experiments, $^*P < 0.05$. (*D*) Western blots for CaMKIIδ protein from cardiomyocytes transfected with miR-675 mimics or antimiR-675. (*E*) Quantitative analysis of fold change in expression of CaMKIIδ under different treatments. $n = 4$ independent experiments, $^*P < 0.05$.

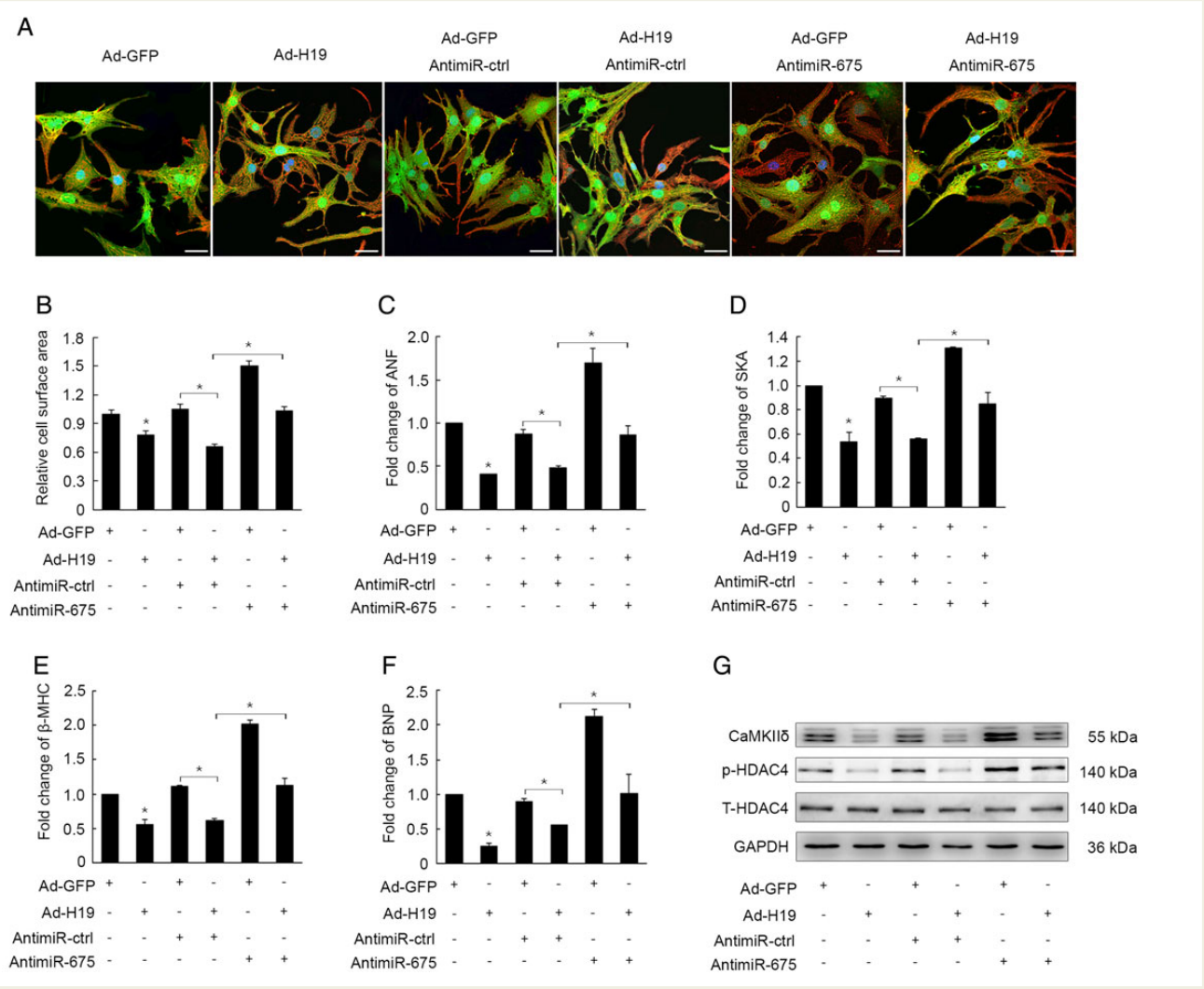

Figure 5 miR-675 mediated the anti-hypertrophic effect of H19 on cardiomyocytes. (*A*) Isolated neonatal cardiomyocytes were infected with Ad-H19 or control adenovirus and treated with or without antimiR-675. Cardiomyocytes were stained for GFP (green) and α-actinin (red). The scale bar represents 40 μm. (*B*) Administration of antimiR-675 rescued the inhibited hypertrophic growth of cardiomyocytes induced by H19 overexpression. Fold change in mean cell surface area of α-actinin-immunostained cardiomyocytes infected with adenoviruses (250 cells per condition; $n = 4$). $^*P < 0.05$. (*C*–*F*) Real-time PCR showed that miR-675 inhibition rescued the down-regulation of foetal genes induced by H19 overexpression. $n = 5$ independent experiments, $^*P < 0.05$. (*G*) Detection of CaMKIIδ and its downstream HDAC4 in different groups by western blot.

cardiomyocytes (see Supplementary material online, *Figure S4A*). When simultaneously knocking down CaMKIIδ (see Supplementary material online, *Figure S4B*) and H19 in cardiomyocytes, we found that CaMKIIδ down-regulation partially overcame the enhanced cardiomyocyte hypertrophy due to H19 inhibition, as measured by the morphological analysis of cardiomyocytes and foetal genes expression (*Figure 6C–G*). These results suggested that CaMKIIδ partially reversed the anti-hypertrophic action of H19 in cardiomyocytes.

3.7 Inhibition of miR-675 exacerbates cardiac hypertrophy in a TAC mouse model

To test the function of H19-miR-675 *in vivo*, we injected antagomiR-675 into mice subjected to pressure overload of the left ventricle by TAC and followed the disease for additional 3 weeks (*Figure 7A*). H19 and miR-675 were all found to be up-regulated in ventricles from TAC-operated mice (see Supplementary material online, *Figure S5A–D*). Considering the fundamental roles of cardiomyocytes and fibroblasts in the heart response against stress, we also detected the expression of H19 and miR-675 in these two cells isolated from sham- or TAC-operated mice, and found that H19 and miR-675 were up-regulated in both cells under the condition of TAC. Although the extent of up-regulation was much more prominent in cardiomyocytes than in fibroblasts (see Supplementary material online, *Figure S5E* and *F*), it could not preclude the possibility that the up-regulation of these two genes in fibroblasts also played important roles in cardiac hypertrophy, and they need to be further investigated in future. TAC-induced miR-675 up-regulation was effectively abolished by antagomiR-675 treatments (*Figure 7B*). Significantly, inhibition of miR-675 enhanced the expression of CaMKIIδ (*Figure 7C*). TAC-operated mice demonstrated significant cardiac hypertrophy, characterized by enlarged heart, higher ratio of LV mass to the body weight (LVM/BW), increased

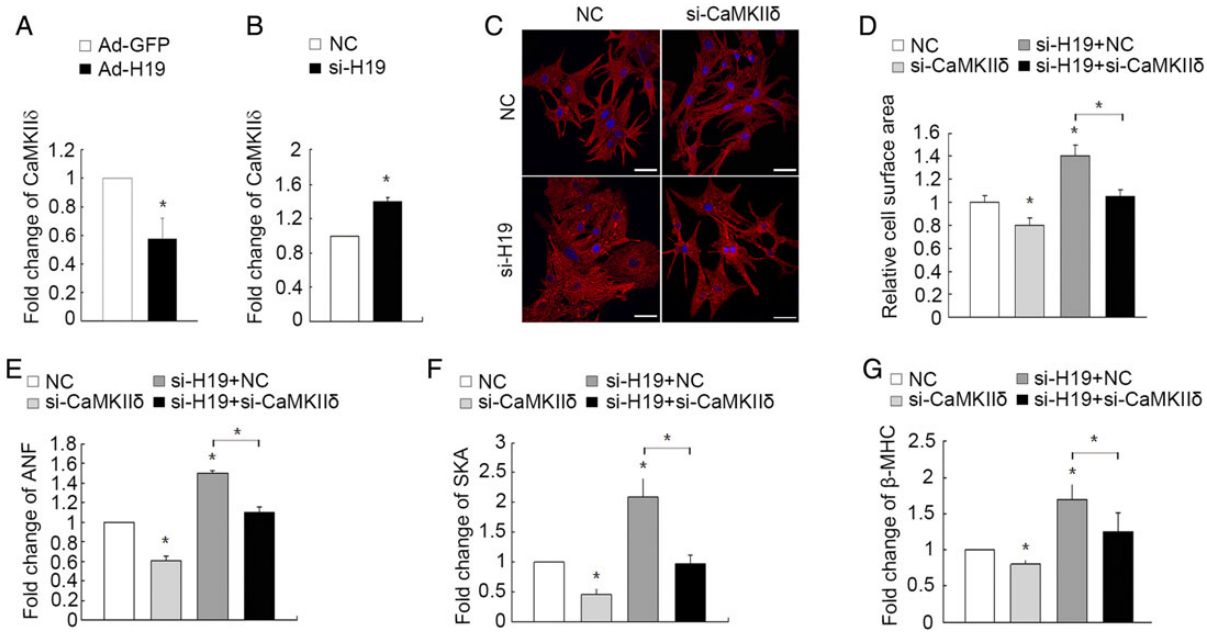

Figure 6 CaMKIIδ partially mediated the effect of H19 on cardiomyocyte hypertrophy. (*A* and *B*) Detection of CaMKIIδ mRNA level in cardiomyocytes by real-time PCR. $n = 5$ independent experiments, $^*P < 0.05$. (*C*) Isolated neonatal cardiomyocytes were infected with si-H19 together with NC or si-CaMKIIδ. Cardiomyocytes were stained for α-actinin (red) and Hoechst (blue). The scale bar represents 40 μm. (*D*) Fold change in mean cell surface area of α-actinin-immunostained cardiomyocytes (236 cells per condition; $n = 4$). $^*P < 0.05$. (*E*–*G*) The levels of ANF, SKA, and β-MHC were measured by real-time PCR. Data represent means ± SEM. $n = 5$ independent experiments, $^*P < 0.05$.

cell cross-sectional area, and increased foetal genes expression, while these effects were accentuated in TAC-operated mice treated with antagomiR-675 (*Figure* 7*D*–*G*). All these results indicated that inhibition of miR-675 *in vivo* exacerbates cardiac hypertrophy in a TAC mouse model.

4. Discussion

Recent researches on lncRNAs have renovated our understanding about the regulation of cardiac diseases, but little is known about the function of lncRNAs in cardiac hypertrophy. H19, a non-protein-coding imprinted and maternally expressed lncRNA, is abundant in embryonic tissues of endodermal and mesodermal origin, but is thought to be expressed mainly in skeletal muscle and heart in adults. In contrast to increasing recognition of the role of H19 in tumour genesis[32–34] and myoblast differention,[26,35] how H19 functions in the heart remains unknown. In this study, we investigated the function of H19 in cardiomyocyte hypertrophy and the related molecular mechanisms. The important novel findings of our study are as follows: (i) H19 is up-regulated under stimulation of pathological stresses and inhibits cardiomyocyte hypertrophy both at baseline and in response to PE. (ii) H19-encoded miR-675 inhibits cardiomyocyte hypertrophy. (iii) miR-675 mediates the anti-hypertrophic effect of H19 on cardiomyocytes. (iv) CaMKIIδ is a direct target of miR-675 and partially mediates the effect of H19 on cardiomyocytes. (v) *In vivo* inhibition of miR-675 exacerbates cardiac hypertrophy in a TAC mouse model. Our present work provided the first evidence to reveal that H19-miR-675-CaMKIIδ axis plays an important role in cardiac hypertrophy.

LncRNAs may function through acting as the precursor of miRNAs. H19 has been shown to act as the precursor of miR-675, and miR-675 mediates the function of H19 in several biological processes.[17–19] As expected, we found H19 overexpression up-regulated the expression level of miR-675 in cardiomyocytes, and miR-675 up-regulation inhibited hypertrophic growth of cardiomyocytes. Moreover, we performed a series of rescue experiments to show that either inhibition of miR-675 in H19-overexpressing cells or overexpression of H19 with mutant pre-miR-675 sequences could partially abolish the effect of H19 on cardiomyocytes. Most importantly, we also performed experiment to demonstrate that *in vivo* knock-down of miR-675 accentuated pressure overload-induced cardiac hypertrophy, suggesting the important role of H19-miR-675 axis in inhibiting cardiac hypertrophy.

We identified CaMKIIδ as a downstream target of H19-miR-675 axis in inhibiting hypertrophic growth of cardiomyocytes. CaMKIIδ is a multifunctional serine/threonine protein kinase mainly found in the heart, which can phosphorylate ion channels, transcription factors, signalling molecules, and other membrane proteins that are critical to cardiac electrical activity and structure.[29] CaMKIIδ is the predominant cardiac isoform and has been shown to act as an inducer of cardiac hypertrophy.[29–31,36] Cardiac-specific CaMKIIδ transgenic mice demonstrate significant cardiac hypertrophy, while CaMKIIδ deletion prevents the development of pathological hypertrophy.[30,31] In addition, CaMKIIδ has also been shown to play a critical role in the development of heart failure in part by accumulation of p53 and induction of cardiomyocyte apoptosis in the dilated cardiomyopathy mouse model.[36] In our study, we demonstrated that CaMKIIδ was a direct target of miR-675 in cardiomyocytes. Furthermore, the levels of CaMKIIδ in TAC-operated mouse hearts were also tested and found to be increased in TAC hearts, which was consistent with previous studies.[31] Although miR-675 was up-regulated in hearts from TAC mice, we noticed that the extent of its up-regulation *in vivo* was less than that of *in*

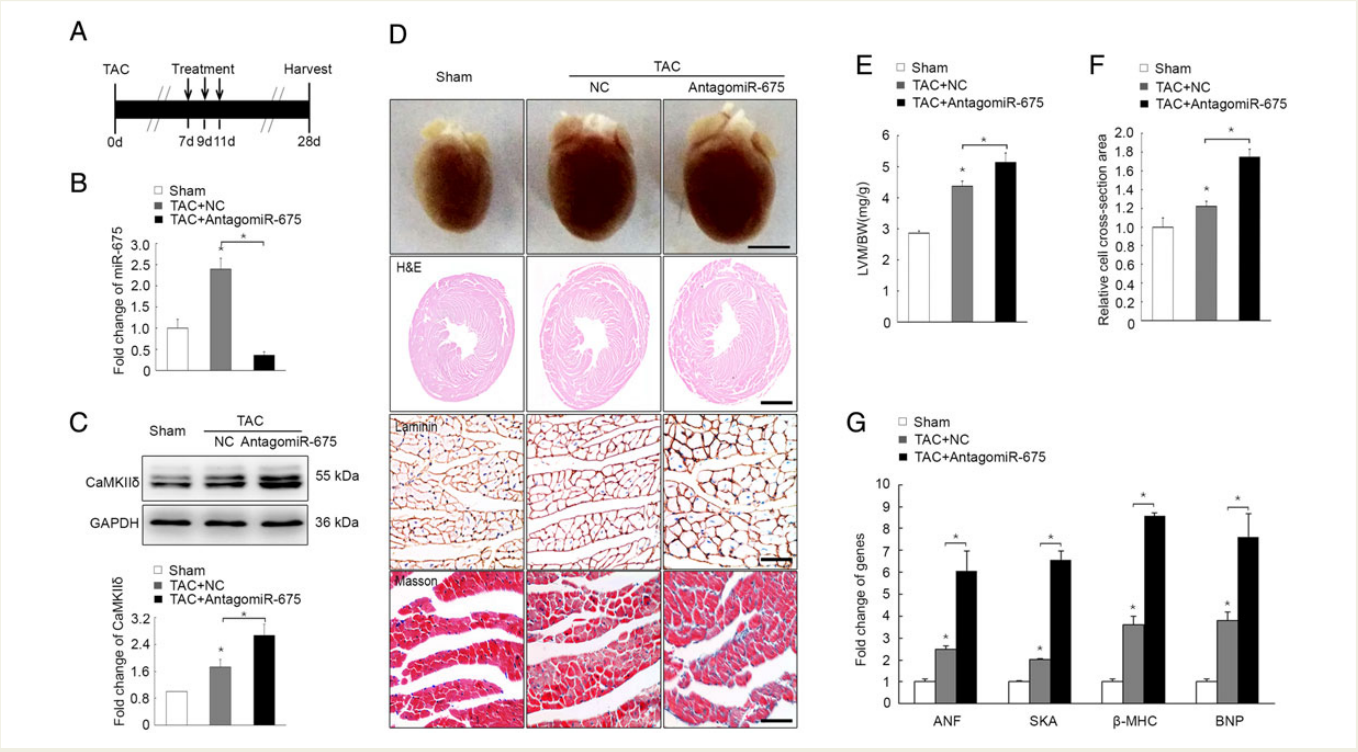

Figure 7 Inhibition of miR-675 exacerbates cardiac hypertrophy in a TAC mouse model. (*A*) Strategy of the therapeutic experiment. (*B*) Detection of miR-675 expression level in a TAC mouse model 21 days after treatment with saline or antagomiR-675. Data represent means ± SEM. $n = 4$ per condition, $^*P < 0.05$. (*C*) Detection (by western blot) and quantitative analysis of CaMKIIδ expression levels in different groups. $n = 3$ independent experiments, $^*P < 0.05$. (*D*) Gross morphology of hearts from different groups (scale bar: 5 mm) and histological analysis of hearts using H&E (scale bar: 2 mm), Masson staining (scale bar: 50 μm), and laminin immunostaining (scale bar: 50 μm). (*E*) Measurements of left ventricular mass/body weight (LVM/BW, mg/g) in different groups. Data represent means ± SEM. $n = 4$ per condition, $^*P < 0.05$. (*F*) Cross-sectional areas were analysed after laminin immunostaining. $n = 400$ cells per condition, $^*P < 0.05$. (*G*) Analysis of the transcripts for ANF, BNP, β-MHC, and SKA by real-time PCR. Data represent means ± SEM. $n = 4$ per condition, $^*P < 0.05$.

vitro experiments (*Figure 1A*; see Supplementary material online, *Figure S2D*), which might lead to insufficient inhibition of CaMKIIδ in TAC mouse model. On the other hand, CaMKIIδ can be activated by many other molecules, which might conquer the inhibitory effect of miR-675 on CaMKIIδ in response to pressure overload. *In vivo* inhibition of miR-675 in TAC mice could enhance the up-regulation of CaMKIIδ and accentuate the cardiac hypertrophy, verifying that miR-675 might inhibit cardiomyocyte hypertrophy by targeting CaMKIIδ. Supportively, CaMKIIδ was down-regulated by H19 overexpression, and inhibition of CaMKIIδ could partially rescue the cardiomyocyte phenotype caused by H19 inhibition, indicating that miR-675-regulated CaMKIIδ might mediate H19-induced inhibition of cardiomyocyte hypertrophy. In this context, our studies provided an important insight into how H19's function in cardiac hypertrophy was mediated by the miRNAs embedded within.

Altogether, our results revealed a novel function of H19-miR-675 axis targeting CaMKIIδ as a negative regulator of cardiomyocyte hypertrophy, providing new insights for understanding the function of lncRNAs in pathogenesis of cardiac hypertrophy.

Supplementary material

Supplementary material is available at *Cardiovascular Research* online.

Conflict of interest: none declared.

Funding

This work was supported by the Chinese National Key Program on Basic Research (2012CB945103), National Natural Science Foundation of China (31430057, 31301203, 81530009, and 81370292) and Beijing Natural Science Foundation (7152049).

References

1. Frey N, Olson EN. Cardiac hypertrophy: the good, the bad, and the ugly. *Annu Rev Physiol* 2003;**65**:45–79.
2. Harvey PA, Leinwand LA. The cell biology of disease: cellular mechanisms of cardiomyopathy. *J Cell Biol* 2011;**194**:355–365.
3. Lyon RC, Zanella F, Omens JH, Sheikh F. Mechanotransduction in cardiac hypertrophy and failure. *Circ Res* 2015;**116**:1462–1476.
4. Braunwald E. The war against heart failure: the Lancet lecture. *Lancet* 2015;**385**:812–824.
5. Rinn JL, Chang HY. Genome regulation by long noncoding RNAs. *Annu Rev Biochem* 2012;**81**:145–166.
6. Fatica A, Bozzoni I. Long non-coding RNAs: new players in cell differentiation and development. *Nat Rev Genet* 2014;**15**:7–21.
7. Ulitsky I, Bartel DP. lincRNAs: genomics, evolution, and mechanisms. *Cell* 2013;**154**:26–46.
8. Flynn RA, Chang HY. Long noncoding RNAs in cell-fate programming and reprogramming. *Cell Stem Cell* 2014;**14**:752–761.
9. Klattenhoff CA, Scheuermann JC, Surface LE, Bradley RK, Fields PA, Steinhauser ML, Ding H, Butty VL, Torrey L, Haas S, Abo R, Tabebordbar M, Lee RT, Burge CB, Boyer LA. *Braveheart*, a long noncoding RNA required for cardiovascular lineage commitment. *Cell* 2013;**152**:570–583.
10. Grote P, Wittler L, Hendrix D, Koch F, Währisch S, Beisaw A, Macura K, Bläss G, Kellis M, Werber M, Herrmann BG. The tissue-specific lncRNA Fendrr is an essential

regulator of heart and body wall development in the mouse. *Dev Cell* 2013;**24**:206–214.
11. Haddad F, Qin AX, Bodell PW, Zhang LY, Guo H, Giger JM, Baldwin KM. Regulation of antisense RNA expression during cardiac MHC gene switching in response to pressure overload. *Am J Physiol Heart Circ Physiol* 2006;**290**:H2351–H2361.
12. Visel A, Zhu Y, May D, Afzal V, Gong E, Attanasio C, Blow MJ, Cohen JC, Rubin EM, Pennacchio LA. Targeted deletion of the 9p21 non-coding coronary artery disease risk interval in mice. *Nature* 2010;**464**:409–412.
13. Wang K, Liu F, Zhou LY, Long B, Yuan SM, Wang Y, Liu CY, Sun T, Zhang XJ, Li PF. The long noncoding RNA CHRF regulates cardiac hypertrophy by targeting miR-489. *Circ Res* 2014;**114**:1377–1388.
14. Han P, Li W, Lin CH, Yang J, Shang C, Nurnberg ST, Jin KK, Xu W, Lin CY, Lin CJ, Xiong Y, Chien HC, Zhou B, Ashley E, Bernstein D, Chen PS, Chen HS, Quertermous T, Chang CP. A long noncoding RNA protects the heart from pathological hypertrophy. *Nature* 2014;**514**:102–106.
15. Nordin M, Bergman D, Halje M, Engström W, Ward A. Epigenetic regulation of the Igf2/H19 gene cluster. *Cell Prolif* 2014;**47**:189–199.
16. Ragina NP, Schlosser K, Knott JG, Senagore PK, Swiatek PJ, Chang EA, Fakhouri WD, Schutte BC, Kiupel M, Cibelli JB. Downregulation of H19 improves the differentiation potential of mouse parthenogenetic embryonic stem cells. *Stem Cells Dev* 2012;**21**:1134–1144.
17. Zhu M, Chen Q, Liu X, Sun Q, Zhao X, Deng R, Wang Y, Huang J, Xu M, Yan J, Yu J. LncRNA H19/miR-675 axis represses prostate cancer metastasis by targeting TGFBI. *FEBS J* 2014;**281**:3766–3775.
18. Keniry A, Oxley D, Monnier P, Kyba M, Dandolo L, Smits G, Reik W. The H19 lincRNA is a developmental reservoir of miR-675 that suppresses growth and Igf1r. *Nat Cell Biol* 2012;**14**:659–665.
19. Gao WL, Liu M, Yang Y, Yang H, Liao Q, Bai Y, Li YX, Li D, Peng C, Wang YL. The imprinted H19 gene regulates human placental trophoblast cell proliferation via encoding miR-675 that targets Nodal Modulator 1 (NOMO1). *RNA Biol* 2012;**9**:1002–1010.
20. Li D, Chen G, Yang J, Fan X, Gong Y, Xu G, Cui Q, Geng B. Transcriptome analysis reveals distinct patterns of long noncoding RNAs in heart and plasma of mice with heart failure. *PLoS One* 2013;**8**:e77938.
21. Sun L, Zhang Y, Zhang Y, Gu Y, Xuan L, Liu S, Zhao X, Wang N, Huang L, Huang Y, Zhang Y, Ren L, Wang Z, Lu Y, Yang B. Expression profile of long non-coding RNAs in a mouse model of cardiac hypertrophy. *Int J Cardiol* 2014;**177**:73–75.
22. Lee JH, Gao C, Peng G, Greer C, Ren S, Wang Y, Xiao X. Analysis of transcriptome complexity through RNA sequencing in normal and failing murine hearts. *Circ Res* 2011;**109**:1332–1341.
23. Wang K, Sun T, Li N, Wang Y, Wang JX, Zhou LY, Long B, Liu CY, Liu F, Li PF. MDRL lncRNA regulates the processing of miR-484 primary transcript by targeting miR-361. *PLoS Genet* 2014;**10**:e1004467.
24. O'Connell TD, Rodrigo MC, Simpson PC. Isolation and culture of adult mouse cardiac myocytes. *Methods Mol Biol* 2007;**357**:271–296.
25. Wang J, Song Y, Zhang Y, Xiao H, Sun Q, Hou N, Guo S, Wang Y, Fan K, Zhan D, Zha L, Cao Y, Li Z, Cheng X, Zhang Y, Yang X. Cardiomyocyte overexpression of miR-27b induces cardiac hypertrophy and dysfunction in mice. *Cell Res* 2012;**22**:516–527.
26. Dey BK, Pfeifer K, Dutta A. The H19 long noncoding RNA gives rise to microRNAs miR-675-3p and miR-675-5p to promote skeletal muscle differentiation and regeneration. *Genes Dev* 2014;**28**:491–501.
27. Guo SL, Ye H, Teng Y, Wang YL, Yang G, Li XB, Zhang C, Yang X, Yang ZZ, Yang X. Akt-p53-miR-365-cyclin D1/cdc25A axis contributes to gastric tumorigenesis induced by PTEN deficiency. *Nat Commun* 2013;**4**:2544.
28. Wang J, Wang Y, Wang Y, Ma Y, Ylan Y, Yang X. TGF-β regulated miR-29 promotes angiogenesis through targeting PTEN in endothelium. *J Biol Chem* 2013;**288**:10418–10426.
29. Anderson ME, Brown JH, Bers DM. CaMKII in myocardial hypertrophy and heart failure. *J Mol Cell Cardiol* 2011;**51**:468–473.
30. Zhang T, Kohlhaas M, Backs J, Mishra S, Phillips W, Dybkova N, Chang S, Ling H, Bers DM, Maier LS, Olson EN, Brown JH. CaMKIIdelta isoforms differentially affect calcium handling but similarly regulate HDAC/MEF2 transcriptional responses. *J Biol Chem* 2007;**282**:35078–35087.
31. Backs J, Backs T, Neef S, Kreusser MM, Lehmann LH, Patrick DM, Grueter CE, Qi X, Richardson JA, Hill JA, Katus HA, Bassel-Duby R, Maier LS, Olson EN. The delta isoform of CaM kinase II is required for pathological cardiac hypertrophy and remodeling after pressure overload. *Proc Natl Acad Sci USA* 2009;**106**:2342–2347.
32. Lee DF, Su J, Kim HS, Chang B, Papatsenko D, Zhao R, Yuan Y, Gingold J, Xia W, Darr H, Mirzayans R, Hung MC, Schaniel C, Lemischka IR. Modeling familial cancer with induced pluripotent stem cells. *Cell* 2015;**161**:240–254.
33. Luo M, Li Z, Wang W, Zeng Y, Liu Z, Qiu J. Long non-coding RNA H19 increases bladder cancer metastasis by associating with EZH2 and inhibiting E-cadherin expression. *Cancer Lett* 2013;**333**:213–221.
34. Yang F, Bi J, Xue X, Zheng L, Zhi K, Hua J, Fang G. Up-regulated long non-coding RNA H19 contributes to proliferation of gastric cancer cells. *FEBS J* 2012;**279**:3159–3165.
35. Eun B, Sampley ML, Van Winkle MT, Good AL, Kachman MM, Pfeifer K. The Igf2/H19 muscle enhancer is an active transcriptional complex. *Nucleic Acids Res* 2013;**41**:8126–8134.
36. Toko H, Takahashi H, Kayama Y, Oka T, Minamino T, Okada S, Morimoto S, Zhan DY, Terasaki F, Anderson ME, Inoue M, Yao A, Nagai R, Kitaura Y, Sasaguri T, Komuro I. Ca^{2+}/calmodulin-dependent kinase IIdelta causes heart failure by accumulation of p53 in dilated cardiomyopathy. *Circulation* 2010;**122**:891–899.